Exact detection of direct links in networks of interacting dynamical units

Exact detection of direct links in networks of interacting dynamical units

Nicolás Rubido[1,2], Arturo C Martí[2], Ezequiel Bianco-Martínez[1], Celso Grebogi[1], Murilo S Baptista[1] and Cristina Masoller[3]

[1] Institute for Complex Systems and Mathematical Biology, University of Aberdeen, King's College, AB24 3UE Aberdeen, UK
[2] Instituto de Física, Facultad de Ciencias, Universidad de la República, Iguá 4225, Montevideo, 11200, Uruguay
[3] Departament de Física i Enginyeria Nuclear, Universitat Politécnica de Catalunya, Colom 11, E-08222 Terrassa, Barcelona, Spain
E-mail: n.rubido.obrer@abdn.ac.uk, arturomarti@gmail.com, ebiancomartinez@gmail.com, grebogi@abdn.ac.uk, murilo.baptista@abdn.ac.uk and cristina.masoller@gmail.com

Abstract

The inference of an underlying network topology from local observations of a complex system composed of interacting units is usually attempted by using statistical similarity measures, such as cross-correlation (CC) and mutual information (MI). The possible existence of a direct link between different units is, however, hindered within the time-series measurements. Here we show that, for the class of systems studied, when an abrupt change in the ordered set of CC or MI values exists, it is possible to infer, without errors, the underlying network topology from the time-series measurements, even in the presence of observational noise, non-identical units, and coupling heterogeneity. We find that a necessary condition for the discontinuity to occur is that the dynamics of the coupled units is partially coherent, i.e., neither complete disorder nor globally synchronous patterns are present. We critically compare the inference methods based on CC and MI, in terms of how effective, robust, and reliable they are, and conclude that, in general, MI outperforms CC in robustness and reliability. Our findings could be relevant for the construction and interpretation of functional networks, such as those constructed from brain or climate data.

1. Introduction

Inferring the underlying topology of a complex system from observed data is currently the object of intense research. However, the limits for the exact inference of direct links in real-world systems composed by interacting dynamical units are still not fully understood. Understanding this limitations is often crucial in many applications in social and natural sciences. In order to infer the underlying network, usually, the observed data comes from time-series recorded at the different units. Then, a direct link between units is assumed depending on how interdependent these observations are. For example, by recording the activity of different brain regions, one wishes to infer which are the relevant structural or functional brain connections by comparing similarity patterns [1–3]. In general, the outcome is a complex network [4, 5] that interconnects the individual units and allows for a better understanding of the overall system behavior.

The main statistical tools used to determine the interdependence of the units have been the cross-correlation (CC) and the mutual information (MI) between their dynamical trajectories [6–16]. Depending on the field of application, the choice of similarity estimators is wider and includes partial correlations, graphical models, and adapted estimators, such as event synchronization [17] (recently used to analyze the summer monsoon rainfall over the Indian peninsula [18]) or response dynamics [19, 20]. However, any similarity measure used to compare two time-series usually results in a non-zero value [21–25]. A reason for this is that, in finite data sets, the presence of persistent trends and/or deterministic recurrent oscillations results in spurious correlations [26–28]. Therefore, network reconstruction methods use fixed link densities (where only the strongest similarity estimates are retained as links, e.g. in [29–31]), link weights (where links are weighted based on the similarity [32]) or pairwise significance tests [33] to ensure the link representativeness. Another reason, which is the focus of our work, is the network connectivity. In particular, the existence of teleconnections [33] (name given in paleoecology to the long-range connections) in systems with multiple/continuous coupling structures result in high similarity estimates between distant nodes. Moreover, even after detrending a data set, the connectivity of the underlying network topology still plays a major role in the non-zero values of the similarity measures between nodes if the network is connected.

Indeed, in undirected connected complex networks, which are the focus of this work, every pair of units is joined by some path. Consequently, any pair of units will exchange some level of correlation or information due to the overall connecting topology. Therefore, the ability to detect a *direct* link between any two units is hindered within the similarity measured value.

Nevertheless, when the links are homogeneous, one expects that directly connected units have larger values of the similarity measure than indirectly connected ones[4]. Then, the existence of a certain threshold, τ, that can split the similarity values into two sets can be expected. If a similarity value between two units is larger than τ, it is considered to be significant and a consequence of a direct link between the two units. Otherwise, it is less significant and a consequence of the lack of a direct link between the two units. A similar method is used in paleoecology to select good modern analog samples for climate and environmental reconstruction [34, 35]. When the strengths of the links are heterogeneous, the weak links are further hindered within the similarity measure values and a bivariate analysis can be insufficient [3]. Moreover, in the presence of strong coupling, global patterns in the system's behavior emerge, creating an effective topology which makes the underlying network inference process unfeasible. Similarly, inference fails for very weak couplings, where the system is hard to distinguish from being composed of uncoupled units. We find that avoiding such fully coherent (large coupling strengths) or incoherent (small coupling strengths) behavior is critical for the detection of the direct links (as it was also found in [20]).

Since different topologies are inferred for different τ values, the problem of finding the optimal τ value which recovers the largest portion of the underlying network is far from trivial. For example, in [12] the presence of dynamical noise in the individual units was shown to enable the identification of an optimal threshold giving an accurate prediction of a network topology, based solely on the measurement of dynamical correlations. However, the method requires computing the inverse matrix of the dynamical correlation matrix, which can be computationally demanding, and also the influence of non-additive noise and/or observational noise remains an open question. Other methods for link identification are based on perturbing the individual units. For example, the method proposed in [36] requires performing independent, simultaneous, and random phase resettings in all the units, which can be impractical in many real-world systems (such as in [29–33, 37]).

In this work, we show that, when the ordered values of CC (computed in absolute value, i.e., the Pearson coefficient) and/or MI (computed via ordinal pattern analysis [38–41]) exhibit a discontinuous curve, an adequate τ value permits inference of *underlying topologies without errors*. The exact link detection is demonstrated by considering various discrete-time dynamical units (logistic maps, circle maps, etc) that mutually interact in different coupling topologies, including random networks (RN). This means that, when the discontinuity is observed, both methods are able to infer the exact underlying network topology that interconnects the units from the local time-series measurements. As a result, the topology of the interacting system is directly related to its function. We find that the existence of this τ occurs even when observational noise and heterogeneities (in the links and/or in the units) are present.

Our results are based on a critical comparison of the CC and MI inference methods *effectiveness* (what is the portion of the underlying topology that is reconstructed correctly), *robustness* (how the effectiveness is affected when parameters are changed, namely, the heterogeneity in the map's dynamics or network weights, the coupling strength between maps, and the network size or connectivity), and *reliability* (results yield consistent inferred networks, even when including observational noise and reducing the time-series lengths). We conclude that MI outperforms CC as the most robust, in particular, is the least sensitive to the choice of τ

---

[4] This conjecture, which constitutes the fundamental cornerstone for the inference methodology of many scientific papers [2], is shown to be true in the supplementary data for the connected part of the CC.

value, and reliable measure. To the best of our knowledge, such reliable reconstruction of network topologies without errors, i.e., the most effective scenario, from time-series measurements of discrete-time dynamical units has not been previously obtained.

2. Model and methods

We consider logistic maps, tent maps, circle maps, and novel maps recently proposed [42] for representing nonlinear optical elements (in the following, referred to as *optical maps*). We observe that our method of network inference is not restricted to maps, but it is demonstrated with maps mainly because of two reasons. First, maps are computationally cost-efficient, allowing long time-series simulations, performing robust statistical analysis, and have been widely used to study complex networks of coupled units [43–45]. Second, continuous systems can be represented by maps (for example, there are many maps that represent various types of neurons [45, 46]) or transformed into maps by means of a Poincaré section or a stroboscopic sampling (time-Poincaré). Here, we let the units have a degree of heterogeneity by using non-identical parameters. For the underlying topology, we use RN [47] and small-world networks [48] with homogeneous and heterogeneous weights. These networks are characterized by the number of nodes, N, the connectivity parameter, p, and the weights heterogeneity degree, g (details are provided in the supplementary data[5]).

The behavior of each map is governed by the equation

$$x_{n+1}^{(i)} = (1 - \epsilon)f\left(r_i,\ x_n^{(i)}\right) + \epsilon\sum_{j=1}^{N}\frac{W_{ij}}{\mathrm{d}_i}f\left(r_j,\ x_n^{(j)}\right), \tag{1}$$

where, $f(r, x) = r\,x(1 - x)$, for the logistic map, and $f(r, x) = x + r - 1.1\sin(2\pi\,x) \bmod 1$, for the circle map (for other maps, see supplementary data. r_i is the ith map parameter, ϵ is the coupling strength, W_{ij} accounts for the weight of the link ($W_{ij} = A_{ij}\left(1 + g\,\xi_{ij}\right) = W_{ji}$, where $A_{ij} = A_{ji}$ is the adjacency matrix of the underlying topology, $\xi_{ij} \in [-1,\ 1]$ is an uncorrelated zero-mean uniformly distributed random number, and g is the degree of coupling heterogeneity), and $d_i = \sum_{j=1}^{N} W_{ij}$ is the weighted degree of node i.

N time-series are obtained from the trajectories of the N maps, generated from random initial conditions. Unless otherwise stated, the length of the time-series is $T = 5 \times 10^4$. The similarity measures are computed from these time-series. In particular, the MI is computed from symbolic sequences of ordinal patterns of length $D = 4$ [38–41] (see supplementary data for details).

The *threshold*, τ, used to split the similarity values, is a control parameter that allows to define the *inferred* adjacency matrix, A_τ: $A_{\tau,\,ij} = 1$ if the similarity measure between maps i and j is larger than τ, and $A_{\tau,\,ij} = 0$ otherwise. The *error*, Δ, between the inferred and the true adjacency matrices, is defined by
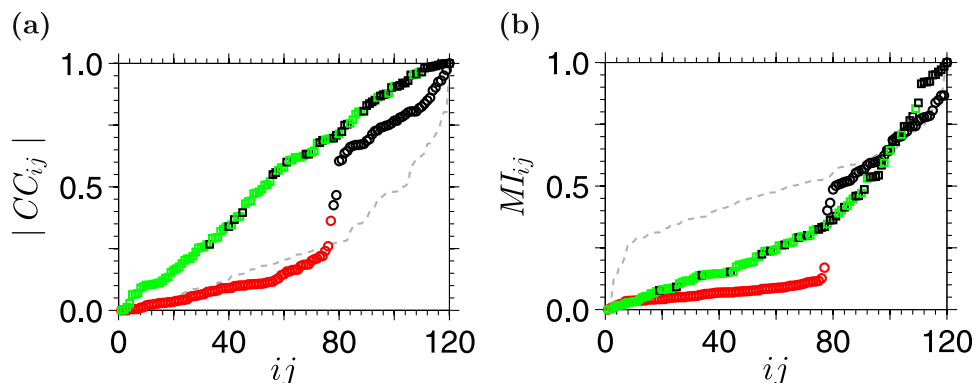
(a)

(b)

Figure 1. (a), (b) shows the normalized CC (MI) values, ordered from smaller to larger values, for all pair of nodes in a weighted ($g = 0.1$) random network ($p = 0.3$) of $N = 16$ identical chaotic ($r_i = 4.0 \ \forall \ i$) logistic maps. The dashed curves (gray online) correspond to the uncoupled situation ($\epsilon = 0$), where no discontinuity is observed. The circles (squares) correspond to a coupling strength of $\epsilon = 0.06$ ($\epsilon = 0.5$), where the values for direct links are signaled by dark—black online—circles (squares) and the values for indirect links are signaled by light—red (green) online—circles (squares). The discontinuity is again absent for $\epsilon = 0.5$ due to the coherent dynamical behavior (synchronous orbits) that the system exhibits at this stage.

$$\Delta = \frac{\sum_{i,j=1}^{N} \left| A_{ij} - A_{\tau,ij} \right|}{N(N-1)} \ . \tag{2}$$

The minimum value of Δ is 0, which corresponds to an exact detection of the true underlying topology. The maximum value of Δ is 1, and occurs only if all the links are inferred incorrectly.

The *effectiveness* of a similarity measure (CC or MI) is quantified by the error Δ between the true topology and the inferred topology, which is a function of the particular threshold τ chosen. We also consider the receiver operating characteristic (ROC) curve, which quantifies the true positive rate (TPR) and false positive rate (FPR), each measure being a function of τ [25] [6]. We consider that a measure is effective when $\Delta \simeq 0$, the TPR is maximum, and the FPR is minimum. The *robustness* of the CC or MI is quantified in terms of how sensitive Δ is to changes in the system's parameters (map's parameter, network topology, and heterogeneity degree) and choice of τ value. We also analyze how Δ depends on the length of the time-series, the level of observational noise, and the size of the network. We consider that a measure is robust, when small changes to the system's parameters or optimal τ value keep $\Delta \simeq 0$. The *reliability* of a method is the ability to give consistently similar results from similar observations; hence, a measure's reliability gives an estimation of the reproducibility of the results.

---

[6] The TPR is defined as the ratio between the number of links that are correctly inferred and the number of links that actually exist in the network. The FPR is defined as the ratio between the number of links that are incorrectly inferred and the actual number of non-existing links in the network. More details are presented in the supplementary data.
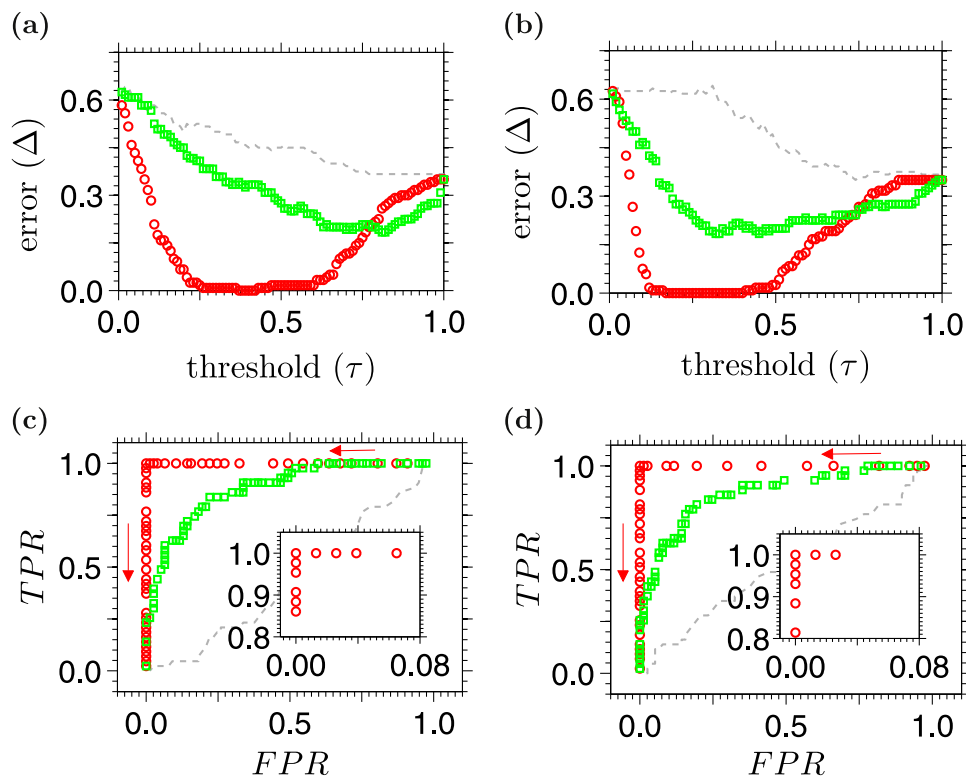
Figure 2. (a), (b) shows the CC (MI) inference error, Δ, as a function of the different threshold, τ, values for the curves and systems of figure 1 (light—gray online—dashed line for $\epsilon = 0$, dark—red online—circles for $\epsilon = 0.06$, and dark—green online—squares for $\epsilon = 0.5$). The corresponding ROC curves are shown in panel (c), (d), where the arrows indicate the direction in which τ increases. The insets in these panels are a zoomed view of the upper left corner of the ROC diagram, showing that for $\epsilon = 0.06$, both similarity measures achieve a perfect inference.

3. Results

In the following we present results for chaotic logistic maps ($r = 4$) and circle maps ($r = 0.35$) coupled in RNs with $N = 16$ and $g = 0.1$. Results for other maps, coupled with other network topologies and heterogeneity degrees, are found in the supplementary data.

Figure 1 shows the ordered values of the normalized CC (figure 1(a)) and MI (figure 1(b)) measures for a particular RN ($p = 0.3$) of identical ($\delta r = 0$) logistic maps coupled with $\epsilon = 0.06$ (circles) and $\epsilon = 0.5$ (squares). Discontinuous curves are found for both, CC and MI, for $\epsilon = 0.06$, though, the gap for MI is larger than the one for CC. We observe that in this case the direct connections (indicated by darker—black online—symbols) are found to have large similarity values, while the indirect connections (indicated by lighter—green online—symbols) have lower values. For comparison, the CC/MI values for $\epsilon = 0$ are shown in light—gray online—dashed lines.

As a general result, we note that the effectiveness of a similarity measure to infer the underlying topology relies on the existence of a discontinuous jump in its ordered values. The abrupt change corresponds to a difference between the values of the similarity measure for direct connections and the values for indirect connections. Specifically, we find that if a gap in
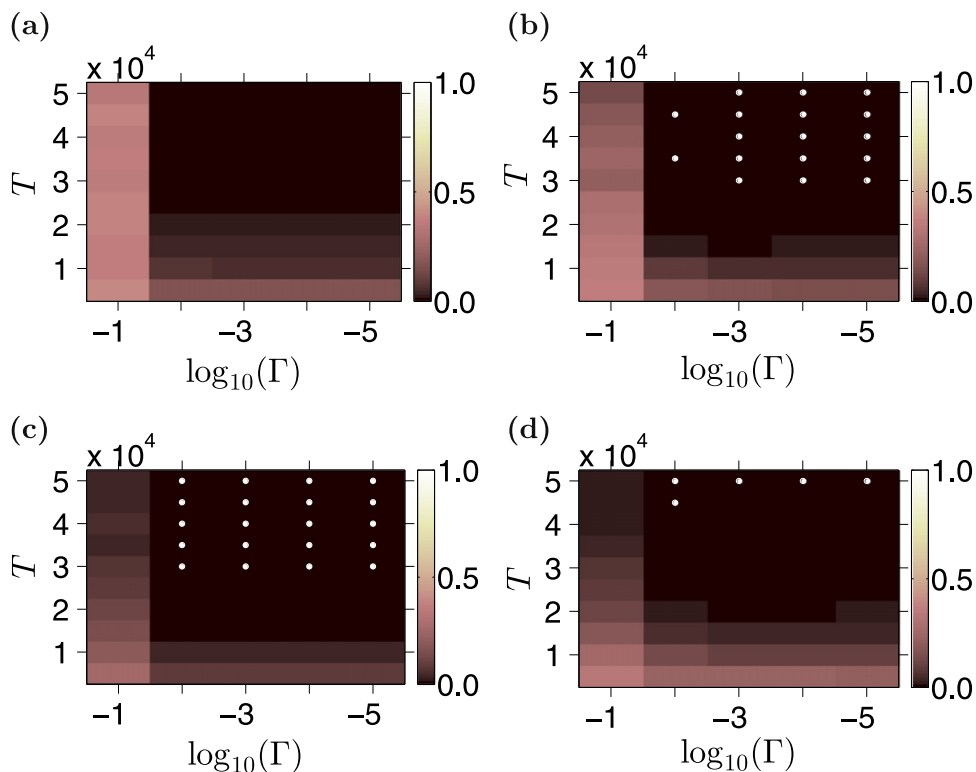
(a)

(b)

(c)

(d)

Figure 3. Minimal error (min (Δ), in color code) values that are obtained from CC (panels (a) and (c)) and MI (panels (b) and (d)) measures of identically ($\delta r = 0$) chaotic logistic maps (top row) and circle maps (bottom row), averaged over five RN realizations (each with equal network characteristics: $p = 0.3$, $N = 16$, and $g = 0.1$), as a function of the observational noise intensity (Γ) added to the times-series and its length (T). We set $\epsilon = 0.06$ for the logistic maps (as in figures 1 and 2) and $\epsilon = 0.12$ for the circle maps. The white dots indicate where an exact detection of all the underlying links is possible in all network realizations, i.e., min (Δ) = 0.

the ordered sequence of CC or MI values exists, any value of τ within this gap infers the underlying topology without errors. When the gap is missing (as for $\epsilon = 0.5$), the direct and indirect connection values are mixed within a continuous curve (represented by squares in figure 1), hence, the error $\Delta > 0$ for any τ value. We find that a necessary condition for the appearance of the gap is to avoid the fully coherent (large coupling strengths) or incoherent (small coupling strengths) behaviors.

In figures 2(a) and (b) we indeed observe that the optimal choice of τ, namely, when $\Delta = 0$, is achieved for values of τ falling within the discontinuity gap of figures 1(a) and (b), respectively. Hence, figure 2 shows the effectiveness and τ-robustness of the two inference measures (in normalized units) for the same network of coupled maps as in figure 1. The underlying network ($N = 16$ node RN with $p = 0.3$) has $M = 50$ links, out of a total of $M_t = N(N - 1)/2 = 120$ possible links. For $\tau = 0$, the inferred network has a global all-to-all coupling topology (as all normalized CC/MI values are $\geqslant 0$), therefore, the error is the relative number of extra links detected (the false positives), $\Delta_{\tau=0} = (M_t - M)/M_t = 70/120 \simeq 0.58$. For $\tau = 1$, the error is the number of true links missed (the false negatives), and these are all the

links, because the inferred topology is a fully disconnected graph (as all normalized CC/MI values are $\leqslant 1$), therefore, $\Delta_{\tau=1} = M/M_t = 50/120 \simeq 0.42$.

Most importantly, we found that, in general, MI is more robust than CC, in the sense that it is able to recover the underlying topology without errors for more threshold values. This is seen by comparing the lengths of the intervals where $\Delta = 0$ for $\epsilon = 0.06$ between figure 2(a) for CC and figure 2(b) for MI. The wider interval is explained by the existence of a larger gap in the values that the MI curve of circles has in figure 1(b), in contrast to the smaller gap in figure 1(a) (however, for some parameters, CC can be more robust than MI in other aspects, as will be shown in figure 3(c)).

Next, we consider the ROC curves, which quantify the TPR and FPR that each measure has as a function of τ [25]. The ROC curves, shown in figures 2(c) and (d), provide further information about the type of errors made as a function of the threshold. When $\epsilon = 0$, as the threshold increases from $\tau = 0$ to $\tau = 1$, both the TPR and FPR decrease (links are not inferred, regardless if they exist or not). On the contrary, when $\epsilon > 0$, as τ increases, only the FPR decreases, while all the existing links are correctly inferred (the TPR remains constant). When τ is increased above the optimal range of values, then the TPR starts to decrease, as existing links are not inferred (the FPR remains constant).

In situations where the knowledge of the underlying topology is missing, the error Δ (equation (2)), TPR, and FPR, cannot be computed. However, if the ordered values of the CC or MI exhibit a discontinuity gap, as in figure 1, the links can still be divided into two sets. The links at the left of the discontinuity (lower than the threshold value) correspond to indirect connections, while any value at the right reveals a direct link (higher than the threshold value). Every value of CC or MI inside the gap can be chosen as a possible threshold value τ and the width of the gap determines the sensitivity of the method. If the gap in the ordered CC or MI values is absent, the method is not capable to infer the correct topology.

For practical applications in real-world data, it is important to analyze how the measures depend on the length of the data set, and on how noisy the data is. In the following, observational noise is considered by adding uncorrelated zero-mean uniformly distributed noise $\eta^{(i)} \in [-1, 1]$ of strength Γ to each data set.

Figure 3 displays (in color code) how the *minimal error* (i.e., min (Δ), the minimum value of Δ corresponding to an optimal τ) depends on the level of observational noise (Γ) and data availability (T) for the network parameters of figures 1 and 2 for identical ($\delta r = 0$) logistic maps (figures 3(a) and (b)) and circle maps (figures 3(c) and (d)). Furthermore, to make the results reliable, we average the min (Δ) value that is found for each Γ and T among five RN realizations with equal statistical characteristics. For the sake of clarity, the white dots in the darker regions indicate where min $(\Delta) = 0$, i.e., the perfect reconstruction of all the RNs.

We can see that MI infers exactly all the network realizations for moderate noise strengths ($\Gamma < 0.1$) and orbits with $T \geqslant 3 \times 10^4$ for the logistic maps (white dots in figure 3(b)) and $T \geqslant 5 \times 10^4$ for the circle maps (figure 3(d)). However, we find that CC fails to provide reliable results for the logistic maps, as it only infers the underlying topology for some RN realizations (dark color in figure 3(a)). On the other hand, CC outperforms MI for circle maps (white dots in figure 3(c)). In general, we note that both methods are effective for moderate Γ and g when sufficient data is available.

Next we show that the exact detection of direct links is also possible when the individual units are heterogeneous ($\delta r = 0.1$), for a wide range of RN parameters and coupling strengths. This can be seen in figure 4, that displays the min (Δ) (in color code) as a function of the
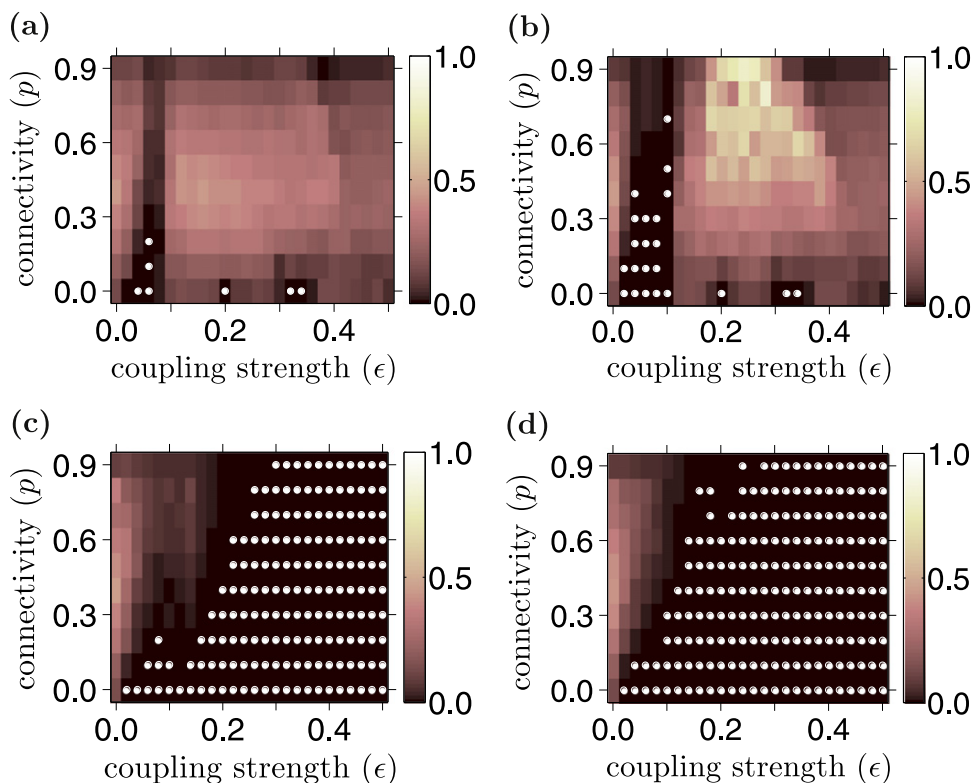
Figure 4. Min (Δ) values averaged (color code) over five unweighed ($g = 0$) RN realizations with equal characteristics obtained from CC (panels (a) and (c)) and MI (panels (b) and (d)) measures for $N = 16$ non-identical ($\delta r = 0.1$) chaotic logistic (top row) and circle (bottom row) maps as a function of the network's connectivity parameter p and coupling strength ϵ. White dots indicate where min $(\Delta) = 0$ in all networks.

connectivity (p) and the coupling strength (ϵ). Each value of min (Δ) is averaged over five network realizations. Results for such parameter space for other maps and topologies are presented in the supplementary data.

Specifically, in figure 4 we see how the region where min $(\Delta) = 0$ for fixed N in the ($\epsilon,\ p$) space changes depending on the units dynamical behavior. In particular, we note that with the exception of a robust window located for $\epsilon \in (0.02, 0.10)$ and $p < 0.5$ where fully incoherent behavior is found (dark region in figures 4(a) and (b)), coupled chaotic logistic maps have periodic windows (light region in figure 4(b)) and synchronized behavior (triangular region in the upper corner of figures 4(a) and (b)) which make the inference impossible. On the other hand, no coherent behavior is found for the circle maps in the same ($\epsilon,\ p$) space (figures 4(c) and (d)). Thus, the region where perfect inference is possible (white circles), is mainly limited by the amount of data available (disregarding $\epsilon \sim 0$). The ϵ-robustness of the CC or MI results, depends on the dynamic of the units composing the system and the topology (p). Although, these results are reliable and the methods are effective if dynamical coherence is avoided and sufficient data is available. In order to retrieve similar regions of perfect inference for larger (N) networks, we find that larger data sets are needed (see supplementary data).

A similar conclusion is drawn when analyzing the effect of increasing the networks size N but keeping the time-series length T fixed. Namely, we note that the region in the $(\epsilon, \ p)$ space that perfect inference is possible diminishes as N is increased if T is kept fixed (see supplementary data). Thus, it is expected that an analysis which uses N/T^α constant, with $\alpha > 1$ as the control parameter, maintains the regions of perfect inference in the $(\epsilon, \ p)$ invariant.

4. Conclusions

To conclude, we have shown that the CC coefficient (calculated in absolute value) and the MI (calculated from ordinal patterns) are able to infer, without errors, the underlying topology of different coupled discrete maps when there is an abrupt change in the ordered set of their magnitudes. We showed that, while both methods require weakly coupled units (avoiding the presence of global patterns, or strong desynchronization) for the abrupt change to exist, the MI is in general more robust and reliable. To the best of our knowledge, reliable reconstruction of network topologies without errors from time-series measurements of discrete-time dynamical units has not been previously obtained.

Various fields where complex networks of interactions are often inferred via a CC or MI statistical similarity analysis of observed time-series can benefit from our results. A careful consideration of the shape of the distribution of similarity values could allow for selecting optimal thresholds for the inference of direct links, as opposite to the often employed methods based on quantiles or on deviations from surrogate data.

Acknowledgements

References

[1] Valencia M, Martinerie J, Dupont S and Chavez M 2008 *Phys. Rev.* E **77** 050905
[2] Bullmore E and Sporns O 2009 *Nat. Rev. Neurosci.* **10** 186–98
[3] Schelter B, Timmer J and Eichler M 2009 *J. Neurosci. Methods* **179** 121–30
[4] Boccaletti S, Latora V, Moreno Y, Chavez M and Hwang D U 2006 *Phys. Rep.* **424** 4
[5] Arenas A, Díaz-Guilera A, Kurths J, Moreno Y and Zhou C S 2008 *Phys. Rep.* **469** 3
[6] Tsonis A A, Swanson K L and Roebber P J 2006 *Bull. Am. Meteorol. Soc.* **87** 585–95
[7] Eguíluz V M, Chialvo D R, Cecchi G A, Baliki M and Apkarian A V 2005 *Phys. Rev. Lett.* **94** 018102
[8] Tsonis A A and Swanson K L 2008 *Phys. Rev. Lett.* **100** 228502
[9] Yamasaki K, Gozolchiani A and Havlin S 2008 *Phys. Rev. Lett.* **100** 228501
[10] Donges J F *et al* 2009 *Europhys. Lett.* **87** 48007
[11] Bialonski S, Horstmann M T and Lehnertz K 2010 *Chaos* **20** 013134
[12] Ren J, Wang W-X, Li B and Lai Y-C 2010 *Phys. Rev. Lett.* **104** 058701
[13] Barreiro M, Martí A C and Masoller C 2011 *Chaos* **21** 013101

[14] Hartman D, Hlinka J, Palus M, Mantini D and Corbetta M 2011 *Chaos* **21** 013119
[15] Berezin Y *et al* 2012 *Sci. Rep.* **2** 666
[16] Tenenbaum J N, Havlin S and Stanley H E 2012 *Phys. Rev.* E **86** 046107
[17] Quiroga R Q, Kreuz T and Grassberger P 2002 *Phys. Rev.* E **66** 041904
[18] Malik N, Bookhagen B, Marwan N and Kurths J 2012 *Clim. Dyn.* **39** 971–87
[19] Timme M 2007 *Phys. Rev. Lett.* **98** 224101
[20] Shandilya S G and Timme M 2011 *New J. Phys.* **13** 013004
[21] Steuer R, Kurths J, Daub C O, Weise J and Selbig J 2002 *Bioinformatics* **18** S231
[22] Panzeri S, Senatore R, Montemurro M A and Petersen R S 2007 *J. Neurophysiol.* **98** 1064–72
[23] Nawrath J, Romano M C, Thiel M, Kiss I Z, Wickramasinghe M, Timmer J, Kurths J and Schelter B 2010 *Phys. Rev. Lett.* **104** 038701
[24] Tchumatchenko T, Geisel T, Volgushev M and Wolf F 2011 *Frontiers in Neurosci.* **5** 8
[25] Hlinka J, Hartman D, Vejmelka M, Runge J, Marwan N, Kurths J and Palus M 2013 *Entropy* **15** 2023–45
[26] Palus M 2007 *Contemp. Phys.* **48** 307
[27] Palus M, Hartman D, Hlinka J and Vejmelka M 2011 *Nonlinear Proc. Geophys.* **18** 751–63
[28] Haam E and Tung K K 2012 *J. Atmos. Sci.* **69** 2934–9
[29] Molkenthin N, Rehfeld K, Marwan N and Kurths J 2014 *Sci. Rep.* **4** 4119
[30] Deza J I, Barreiro M and Masoller C 2013 *Eur. Phys. J. Spec. Top.* **222** 511–23
[31] Feng Q Y and Dijkstra H 2014 *Geophys. Res. Lett.* **41** 541–6
[32] Gozolchiani A, Havlin S and Yamasaki K 2011 *Phys. Rev. Lett.* **107** 148501
[33] Rehfeld K and Kurths J 2014 *Clim. Past* **10** 107–22
[34] Waelbroeck C, Labeyrie L, Duplessy J-C, Guiot J, Labracherie M, Leclaire H and Duprat J 1998 *Paleoceanography* **13** 272–83
[35] Sawada M 2006 *Comput. Geosci.* **32** 818–33
[36] Levnajić Z and Pikovsky A 2011 *Phys. Rev. Lett.* **107** 034101
[37] Runge J, Heitzig J, Marwan N and Kurths J 2012 *Phys. Rev.* E **86** 061121
[38] Bandt C and Pompe B 2002 *Phys. Rev. Lett.* **88** 174102
[39] Amigó J M 2010 *Permutation Complexity in Dynamical Systems-Ordinal Patterns, Permutation Entropy, and All That* (Berlin: Springer)
[40] Zanin M *et al* 2012 *Entropy* **14** 1553
[41] Amigó J M and Keller K 2013 *Eur. Phys. J. Spec. Top.* **222** 263–73
[42] Hagerstrom A M, Murphy T E, Roy R, Hvöel P, Omelchenko I and Schöll E 2012 *Nat. Phys.* **8** 2372
[43] Martí A C, Ponce M and Masoller C 2005 *Phys. Rev.* E **72** 066217
[44] Ponce M, Masoller C and Martí Arturo C 2009 *Eur. Phys. J.* B **67** 83–93
[45] Neiman A, Pei X, Russell D, Wojtenek W, Wilkens L, Moss F, Braun H A, Huber M T and Voigt K 1999 *Phys. Rev. Lett.* **82** 660–3
[46] Ibarz B, Casado J M and Sanjuán M A F 2011 *Phys. Rep.* **501** 1–74
[47] Erdös P and Rényi A 1959 *Publ. Math.* **6** 290–7
[48] Watts D J and Strogatz S H 1998 *Nature* **393** 440–2